Universidad Zaragoza
1542

Facultad de Ciencias
Universidad Zaragoza

Instituto Universitario de Investigación
en Ingeniería de Aragón
Universidad Zaragoza

Trabajo Fin de Grado

Application of holographic microscopy in microchannels

Autor/es

Juan Gracia García-Lisbona

Director/es

Mª Nieves Andrés Gimeno
Virginia R. Palero Díaz

Facultad de Ciencias

Curso 2018/2019

Index

Introduction and objectives

Since mid-1970 magnetic particles have been used for biomedical applications as it is possible to take advantage from their main feature: its reaction to magnetic fields [1]. In addition, as magnetic particles are not toxic, it is possible to directly use them inside the human body for a variety of diseases detection and treatment: Magnetic Resonance Imaging (MRI), hyperthermia (during cancer treatment), drug delivery through the blood current, magnetic separation and blood purification processes. Before implementing those techniques in human beings, it is important to study the behaviour of the particles in the laboratory when similar conditions are applied.

Digital Holography [2] (DH), a non-intrusive technique, is an emerging technology in imaging applications. The remarkable benefits from DH are numerous; an easy and rapidly registration of the data, the total availability of the amplitude and phase information about the complex object wave and the flexibility of the image processing techniques. In DH, the interference between the object beam and the reference beam is recorded in a digital sensor and converted into an array of numbers. Then, the complex amplitude is propagated representing the amplitude and the phase of the complex object wave.

In Digital Holographic Microscopy (DHM), the technique that will be applied during this work, the advantages from DH are implemented over a microscope set-up. One of the distinctive features of holography is the 3D registration of the complex object wave in an hologram in order to reconstruct the optical field at any distance. This technique has been recently applied for numerous biological studies, in both vivo and ex-vivo samples, such as recording living cells (mainly transparent) or microfluidics registration of the circulatory system. In DHM, the diffracted light from the sample is magnified by the microscope objective and the interference between both beams (object and reference) is registered by the digital sensor. The usual optical configuration in DHM is in-line holography. However, in our work an off-axis holographic set-up will be considered

In this work, a new approach to the study of microfluidics will be presented. Microchannels with different width had been designed to study the particle movement under the effect of a magnet.

To prepare and check the correct function of the holographic microscope, different samples will be recorded. First, a series of samples containing arrays with microlenses had been used to check the alignment and the magnifications of the different objectives.

Later on, in order to implement a fluidics system, a sample containing 1mm capillaries will be recorded. Magnetic particles will be observed through the channel and a reconstruction of the complex object wave intensity will be presented.

Finally, the design, preparation and results from the new microchannels will be presented. A microfluidics system will be prepared in order to register magnetic particles moving through a 100-micrometer width capillary. At the end, different reconstruction methods for the object complex amplitude will be analyzed.

1. Holographic microscopy

In 1948, while trying to improve the resolution of the electron microscope, Denis Gabor invented holography [3]. He realized that if the electron image wave was dispersed, instead of trying to improve its resolution, the diffraction pattern of the electron beam (so called dispersed wave) contained complete amplitude and phase information. For that reason, it was possible to recover the original image by using high resolution photographic plates.

Nowadays, the primary photochemical method is consider as "analog holography". It has been replaced by digital holography [4] and consequently, the photographic plates have been substituted by digital sensor cameras with all the advantages of the electronic imaging.

1.1. Introduction to digital holography

In digital holography the interference between two light beams, object beam and reference beam, are recorded by using a digital camera (typically CCD or CMOS sensors). The object beam, O(x,y), comes out from the dispersed light from the object. The reference, R(x,y), comes from the same light source.
The object and reference complex beams can be written as:

$$O(x,y) = A_O \cdot \exp(j \cdot \phi_O(x,y))$$
$$R(x,y) = A_R \cdot \exp(j \cdot \phi_R(x,y)) \quad (1)$$

where A denotes amplitude and ϕ denotes phase. The hologram intensity is given by:

$$I(x,y) = |O(x,y) + R(x,y)|^2$$
$$= |O(x,y)|^2 + |R(x,y)|^2 + R(x,y)^* \cdot O(x,y) + R(x,y) \cdot O(x,y)^* \quad (2)$$

The first two terms in Eq.(2) are the dc terms, the third and fourth terms corresponds to the real and virtual image. It can also be written as follows:

$$I(x,y) = A_O^2 + A_R^2 + 2 \cdot A_R \cdot A_O \cdot \cos(\phi_O - \phi_R) \quad (3)$$

It is shown that the hologram contains complete information about amplitude and phase of the object beam.

Due to the low resolution of the camera sensor, a small angle between both beams is required to record an off-axis hologram. For that reason, a beam cube splitter located in front of the camera is used to combine both beams and

ensure a small angle between them. In order to record a lensless Fourier Transform hologram the source of the divergent reference beam needs to be placed at equal distance from the sensor as the lens aperture used to image the object. A possible setup is shown in Figure 1.

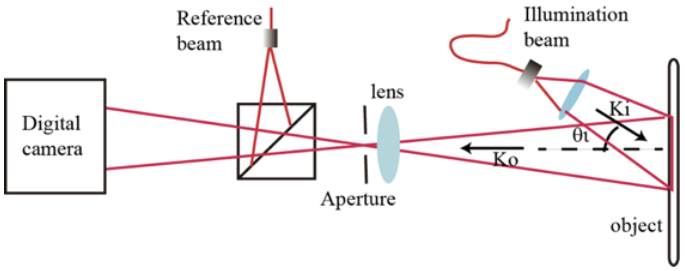

Figure 1. Optical setup for recording of the Fourier Lens less of the aperture.

It is difficult to isolate the real and virtual images from the dc term. However, introducing a spatial phase shifting, all terms are separated in the frequency domain [5]. In order to introduce a liner phase shifting, the origin from the reference beam is displaced a Δr amount from the lens aperture center (Fig. 2a). Thus, to resolve the frequency modulation, the speckle size has to be increased up to a value about 3 pixels. The increse of the speckle size is related with a incresing in the aperture number, limiting the aperture size. The Fourier Transform of the digital hologram (Fig. 2b) shows the dc term in the middle of the image and the real and virtual images of the lens aperture appear centered at a frequency $\pm f_0$, proportional to the reference beam source displacement Δr.

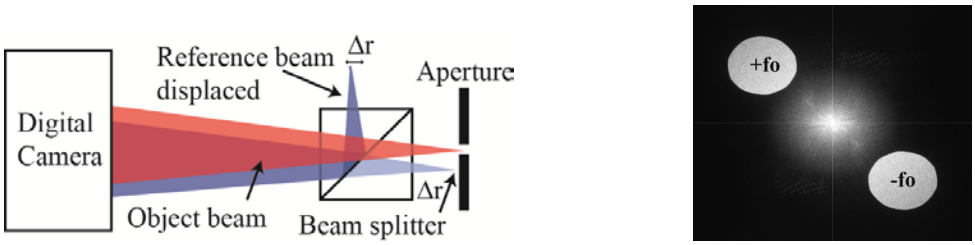

(a) (b)

Figure 2. (a) Optical setup for recording an hologram. (b) Fourier Transform of a registered hologram.

The aperture size can be increased (limited by the speckle size requirements) but it is important not to overlap the aperture images with the dc term to avoid background noise.

The isolation of these terms allows selecting only one of them (real or virtual) for the reconstruction process while the rest of the information is blocked. The selected image is moved to the center of the frequency plane and the inverse Fourier Transform is performed to obtain the object wave. Using the

Convolution Method [5], this wave is propagated to the object plane, where the intensity and phase distributions are reconstructed.

The complex amplitude represents an array of numbers. For that reason, it is possible to obtain different visualizations from it. Mainly, the intensity or the phase of the complex amplitude are presented. However, during the analysis section in this report only intensity representations of the complex amplitude, showing a better contrast, will be plotted. The phase representations (real and angle part) of the complex amplitude did not have enough contrast and the diffraction figures of the particles were not visible.

1.2 Optical setup: holographic microscope

An off-axis digital holographic microscope setup is presented in Figure 3. A solid state laser beam with wavelength, λ=515.4nm, has been used. By using a beam splitter, the laser source is divided in object and reference beams. Both beams are guided through optical fibre. The object beam is collimated by a lens and then, pointed towards the optical axis by a prism. Afterwards, it passes through the object and the diffracted light goes through the microscope objective. Finally, the object beam goes through the beam cube splitter and reaches the digital sensor. The diffraction introduced by the edges of the beam cube splitter is eliminated by using an aperture located around the cube. The divergent reference beam is pointed towards the beam cube splitter where is merged with the object beam. The optical fiber end of the reference is placed at the same distance as the objective lens aperture is from the sensor in order to records a Lens less Fourier hologram (with a imposed Δr so a spatial phase shifting is introduced). The interference of both beams is recorded in the digital sensor. In general, the reference beam intensity is always bigger than the intensity of the object beam.

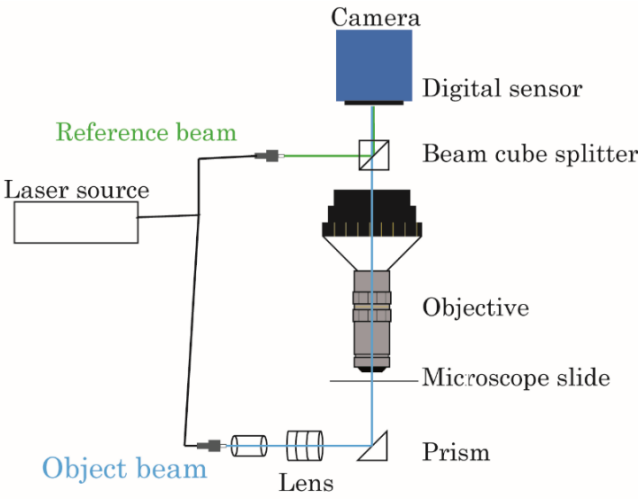

Figure 3. Diagram of the holographic microscope.

Before starting with the measurement process, it was important to check that the object beam direction was centered with the optical axis and the camera sensor was placed perpendicular to the optical axis ($\theta=0$). A perfectly aligned system would allow to change the objective without modifying the alignment. However, in our system when changing between the different magnifications the centering of the object image needs to be checked and slightly centered.

Remark that a 3D volume from the sample is recorded in the digital sensor. For the recording, a selected plane is focussed, but the digitally reconstruction of the hologram allows to reconstruct any other plane in focus. In this kinds of holograms, sensitivity in the Z-axis is much weaker than in the other two axis.

The samples were placed on the microscope plate that is fixed on a Z coordinate and allowed XY movement. To focus the sample the camera should be moved along the Z-axis. That movement always implies a small change in the magnification. For small samples, micrometric Z movements were allowed and the focus image was determined by the motion of an extra stage along the Z-axis, keeping the magnifications constant.

2. Preliminary experiments

In order to get used to the measuring and analysis process as well as with the holographic microscope, a series of objects were firstly observed with the microscope before the capillaries. As a result of this, knowledge about how to manipulate the experimental set-up, software and microscope objects was learned.

A series of samples containing arrays with microlenses were observed as well through the microscope. The samples were fabricated by the Polymers group at the Institute of Material Science in Aragón (ICMA). In each slide, arrays of microlenses were created using a drop by drop ink deposition. Then, in order to fix the lenses over the slide, a treatment was applied. Depending on the number of ink drops, the shape of the created lens was more or less spherical and thus have different size. The main objectives were to record the lenses in an hologram, reconstruct the object wave in order to estimate the focal length, shape and lens diameter and in general, check the experimental setup for further experiments.

Each slide containing microlenses was placed over the microscope plate with tweezers in order to avoid contamination. These samples, mounted on a micrometric Z-stage, movement in three directions was possible. For that reason, the focusing process was performed by moving up or down the sample (moving it closer or away from the camera). By using the 10x objective of the microscope, a series of microlenses were focused and recorded with an exposition time of 35ms. The recorded hologram containing two microlenses is given in Figure 4.

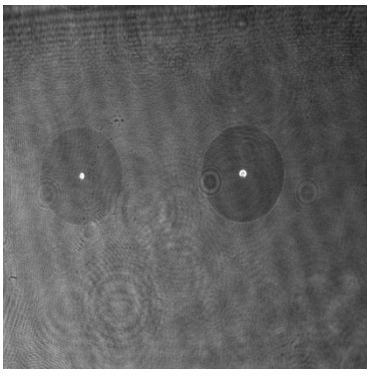

Figure 4. Hologram containing two microlenses.

Then, by reconstructing the object wave it has been possible to obtain the intensity and the phase at any Z position. The analysis of the microlens that appear in the right part of Figure 4 will be presented.

It is important to notice that once the hologram has been recorded, it is possible to reconstruct the object complex amplitude in any plane. In Figure 5(a,b) representations of the microlens at the focusing plane are given. Then, in the following Figures 5 (c,d) the same microlens is represented in an out of focus plane.

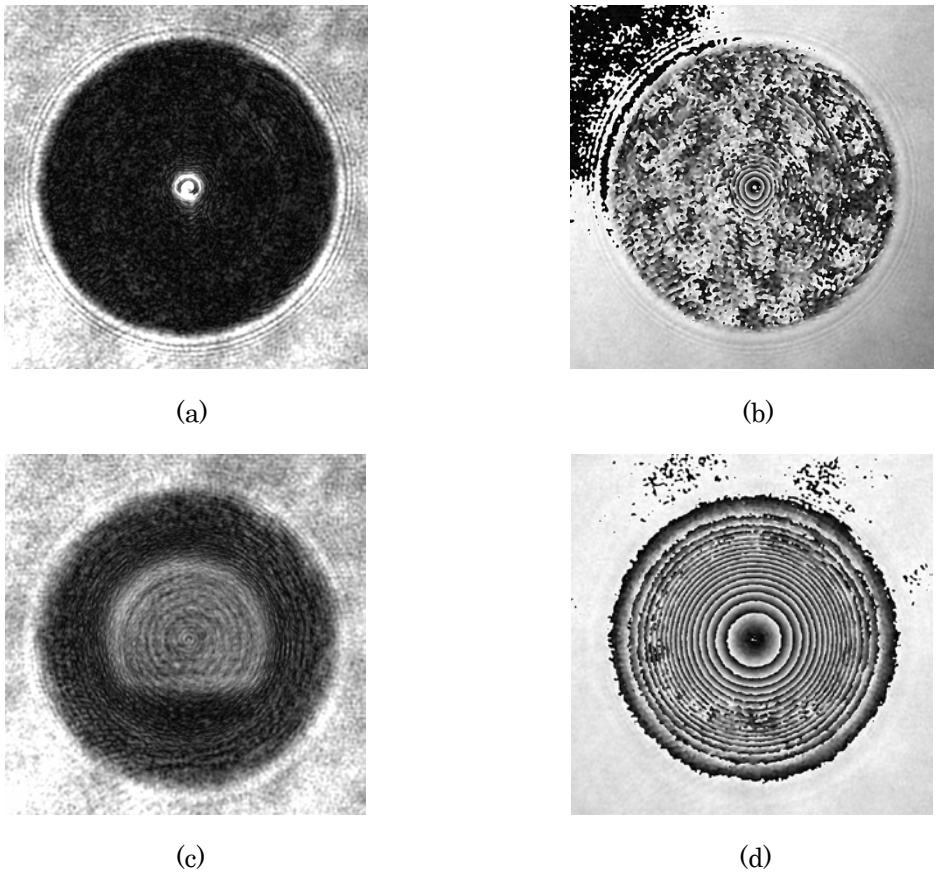

(a) (b)

(c) (d)

Figure 5. (a) Right microlens from Fig.4: intensity representation. (b) Right microlens from Fig.4: phase representation. (c) Out of focus intensity representation. (d) Out of focus phase representation.

The position of the reconstruction plane presented in Figure 5(a) allow to determine the focal lengths defined as the distance at which a beam of collimated light that crosses the lens is focused to a single spot. In addition, the fringe pattern presented in Figure 5(d) will allowed us to determine the shape and the diameter of the microlens. The analysis for the microlens arrays are out of the scope of this work.

Holograms of a system containing microchannels were also recorded. This setup was implemented in order to learn how to manipulate a microfluidics circuit as well as the microparticles.

The sample is made of methacrylate and has three implanted microchannels each of them with volume 1x0,3x20mm3. The microchannel (Fig.6(a)) is filled using a syringe with a mixture of water and glycerine. The fluid was prepared

with 3-micrometer diameter magnetic particles in low concentration previously unsticked. A series of holograms were recorded using the 20x objective and with an exposition time of 100ms. The digital reconstruction of the object image was used to locate the particles over the channel and an intensity representation is given in Figure 6(b).

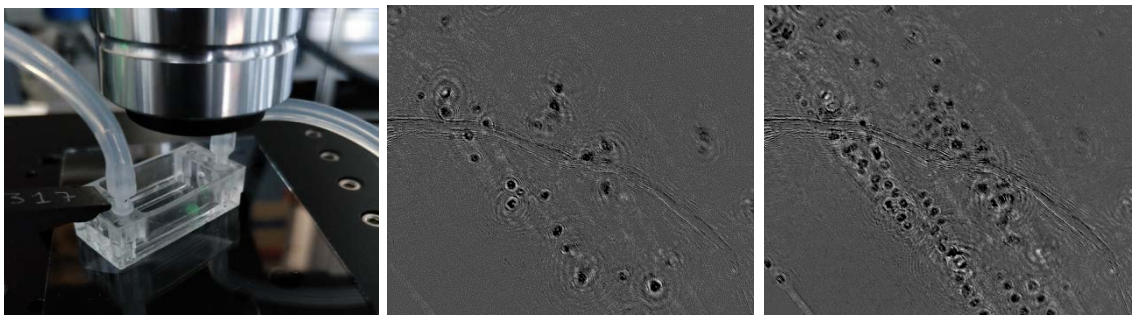

(a) (b) (c)

Figure 6. (a) Microchannel over the microscope slide. (b) Digital reconstruction of the particles. One hologram. (c) Particles traces for the sum of intensities. Sum of five holograms.

Holograms recorded with a ΔT=500ms will be analysed. In order to observe particle motion and velocities inside the capillary it is possible to sum the intensities of the recorded holograms. In Figure 6(c) the intensities of 5 holograms has been presented. As it is possible to observe, the particle traces images are located along the motion direction of the fluid and would allow to determine the velocities.

3. Application to microchannels

The main goal of this work was to record holograms of microchannels. For that reason, a series of microchannels, so-called capillaries, were designed together with BeOnChip [7], a Start-Up of the University of Zaragoza.

Capillaries were created with a lithographic process inside a white room by using deposition of UV rays over an epoxy wafer. The position for the channels was chosen in order set a magnet as close as possible to the chip in further experiments. In the building process capillaries were implanted over a chip, and to take advantage of the wafer, two capillaries were implanted in each chip, in both borders. Two different types of capillaries were designed: straight capillaries (Fig. 7(a)) with 100x100 micrometers (width x depth) and 250x50 micrometers and "chair-size" (Fig. 7(b)) capillaries with 250x250 and 500x250.

(a) (b)

Figure 7. Different capillaries designed for the project. (a) Straight capillary. (b) "Chair size" capillary.

In addition, another two pieces were designed for the capillaries. The first one is the piece that hold the microchannels chip and allow the connection with the fluidics circuit (Fig. 8 Blue). The second one is another piece that ensures that the whole experimental setup is fixed into the microscope (Fig. 8 Green).

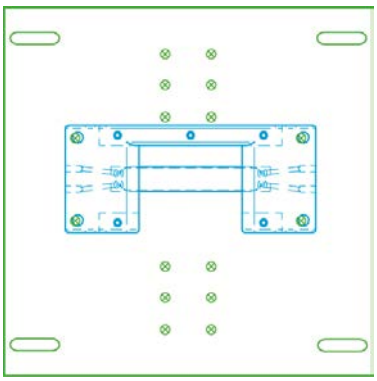

Figure 8. Different stands for the microchannels.

3.1. Design and preparation

In our experiments, the 100x100 capillary was chosen. The main reason for that was that we wanted to check the possibility of observing the magnetic particles moving through the smallest capillary we had.

The chosen liquid was a mixture of pure water and glycerine and there were two reasons for using it. The first one was that as we want to simulate blood circulation, the right choice should be a liquid with similar viscosity with blood. The second one was that the refraction index of the mixture was n=1.4145, similar to the refractive index of the capillary (glass) so the refractions due to medium changes were prevented.

Magnetic particles MagP NH2 (from nanoMyP) were used. Those are made of polyurethane with 5% of magnetite in volume. Here, particles are considered as spheres with an average diameter of 3 micrometres. Magnetic particles were chosen because in further studies the particles will be manipulated while they pass through the capillary under the influence of a magnet. A low concentration of particles was selected for the experiments since the objective was observing single particle traces over the capillary. Once the magnetic particles have been added to the liquid, it was important to place the mixture (kept inside a container) 5 minutes into an ultrasound machine. That step was done in order to avoid particles for sticking together and, as a result of that, damaging the capillary.

To produce a laminar flow, the microfluidics pump Nexus 3000 High FlowSyringe from Chemyx was used [8]. Once the pump is turned on, a servomotor applies pressure on the top of a syringe and the fluid flows through the system. For the experiments, the minimum flow was chosen since it was the first time the capillaries were used.

Syringe (mm)	Volume (ul)	Rate (ul/min)	Delay (min)
4,7300	1000	0,0016	0,0000

Table 1. Pump parameters.

The step by step process that was done in the laboratory for the preparation of the system started by fixing the chip (Fig. 9(a)) into the support piece, always using gloves and tweezers to avoid contamination. It was also important to prevent direct sunlight to fall upon the capillaries. Then the support piece was attached into the methacrylate piece (Fig. 9(b)) that goes directly into the microscope slide (Fig. 9(c)).

It was found easily to connect, by applying pressure, the microfluidics tubes to the support before mounting it into the microscope. For all the connections plastic tubes with diameters 0.08mm (internal) and 2.4mm (external) has been used. Once that was done, a syringe was used carefully to fill tubes and

capillary with the liquid. It was done to balance the levels of pressure over the circuit. Finally, the tube was connected to the syringe and placed on the pump.

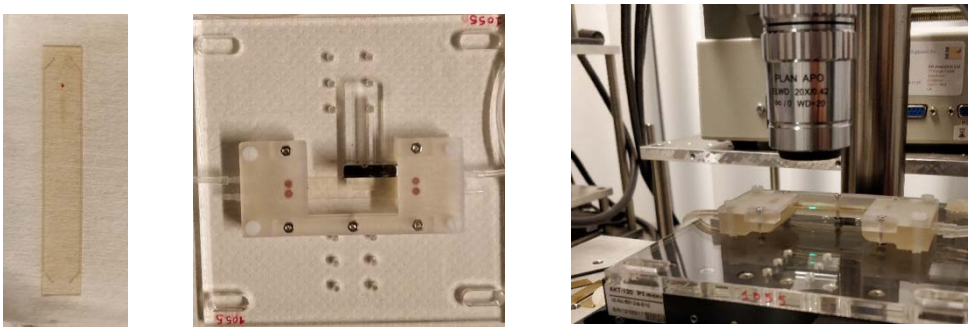

(a) (b) (c)

Figure 9. (a) Microchannel chip. (b) Support and connection pieces for the capillary. (c) Capillary setup over the microscope.

Once the recording process was finished, it was also important to leak out the circuit in order to removing the particles and remaining liquid from it. Using the same syringe, the system was filled with air to empty the tubes and capillary.

3.2. Recording of data

The holographic recording is fully automatized by the computer. CamWare software has been used and the variable parameters were: exposition time that is changed depending on the desired quantity of light, frame rate that is changed depending on the speed of the particles. Besides, the size of the recorded hologram can be changed allowing high-speed recording. In our experiments, the maximum size of the camera, 2560x2160 pixels, will be used. The holographic record allows recording either a single hologram or a 200-hologram series, the usual case.

Several tests were performed with the different recording parameters before selecting the final values used during the report. Finally, all the holograms presented here were 200-hologram series recorded with a frame rate of 49,97fps and an exposure time of 40ms. For all series the reference intensity was recorded.

The holographic recording is performed out of focus. The main reason is that while performing the digital reconstruction of the holograms, the diffraction pattern of the particles should be distributed over an area of some pixels. In order to make that, the particles were focused using a live-view option from

the camera and then, the image was moved out of focus in order to register the hologram.

The used holographic microscope allows changing between 20x, 50x or 100x magnification by switching the objectives, as it is possible to observe in Figure 10. Since it was the first time capillaries were used and we wanted to collect maximum information from the holographic recording, the minimum magnification that allowed to record the whole microchannel was chosen for the recording (20x objective). In the following figure (Fig.10) the different parts from the used holographic microscope are presented.

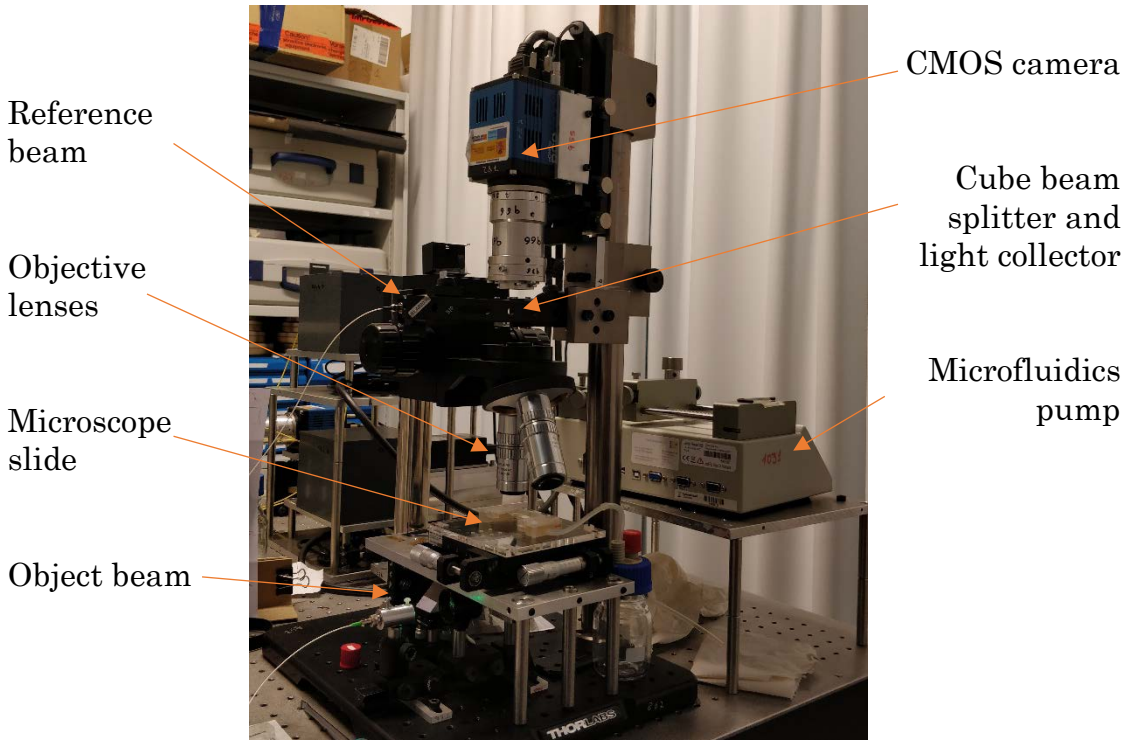

Figure 10. Holographic microscope.

It was also important to obtain a precise approximation of the objective magnifications used that in this case were 20x and 50x. In order to obtain them a single hologram, and the reference beam intensity, was recorded with each objective. Instead of focusing the capillaries, a slide containing different millimetric grids was focused. With its reconstruction (Fig.11) and by measuring the size of the grid both objectives magnifications were obtained. In the case of the 20x objective a 22 magnification was obtained. For the 50x objective, the obtained magnification was 57.5.

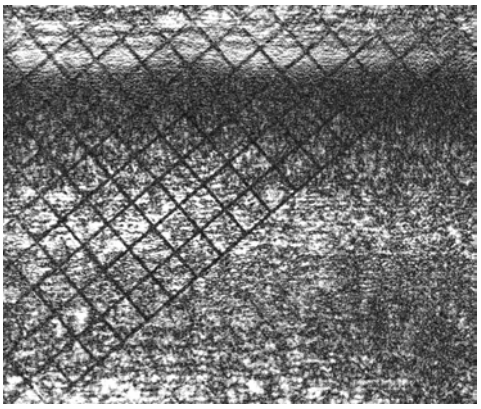

Figure 11. Digital reconstruction of the microscope slide containing the grid.

3.3. Analysis

In this section the analysis and results for the 100-micrometer capillary is presented. The main objectives were to locate and follow the magnetic particles through the microchannel. In addition, by using the trace representation of the particles it will be possible to estimate the speed of different particles.

The maximum recording size is 2560x2100 pixels that in real space becomes 750x620um^2 However, to spend less computational time just the capillary fragment will be analyzed, 2560x500 pixels, that become 750x148um^2 in real space. Furthermore, in some cases just the area of an individual particle trace is processed so the used area is different for each analysis.

All the analysis of the recorded data was performed with MatLab. The used programs are a combination of existent software, that was adapted to analyze capillaries, and new programs that were created for this project while unexpected issues came out.

As off-axis holograms were recorded, the Fourier Transform method has been applied for the analysis of the holograms. The real aperture image is selected in the Fourier plane, centered and the Fourier Transform inverse is applied to obtain the object complex amplitude.

Before performing particle analysis, it is important to remove background noise and possible extra reflections created by the capillary or tiny specks of dirt on the experimental set-up. For that reason, a background is obtained from every 200-hologram (the complete series) or a selection of holograms doing an average of the intensity of the object complex wave.

Once the background has been obtained, it was removed from each analyzed hologram. The Convolution Method is used in order to propagate the complex

amplitude to the plane in which the desired particle is focus. To observe the particles moving through the channel, the intensities of several holograms are summed.

The typical registered hologram is given in Figure 12(a). It is possible to distinguish different diffraction patterns from the reference beam as well as some of the information of the object beam. In order to observe particle movement, the particle images corresponding to different times are presented together in the same image by summing the intensities of the corresponding complex object waves. In Figure 12(b) the reconstructed particle image at the plane z=-0.07mm is presented. The analyzed holograms are recorded every 200ms. In Figure 12(c) it is presented the zoomed area corresponded to the particle trace noted from the previous figure.

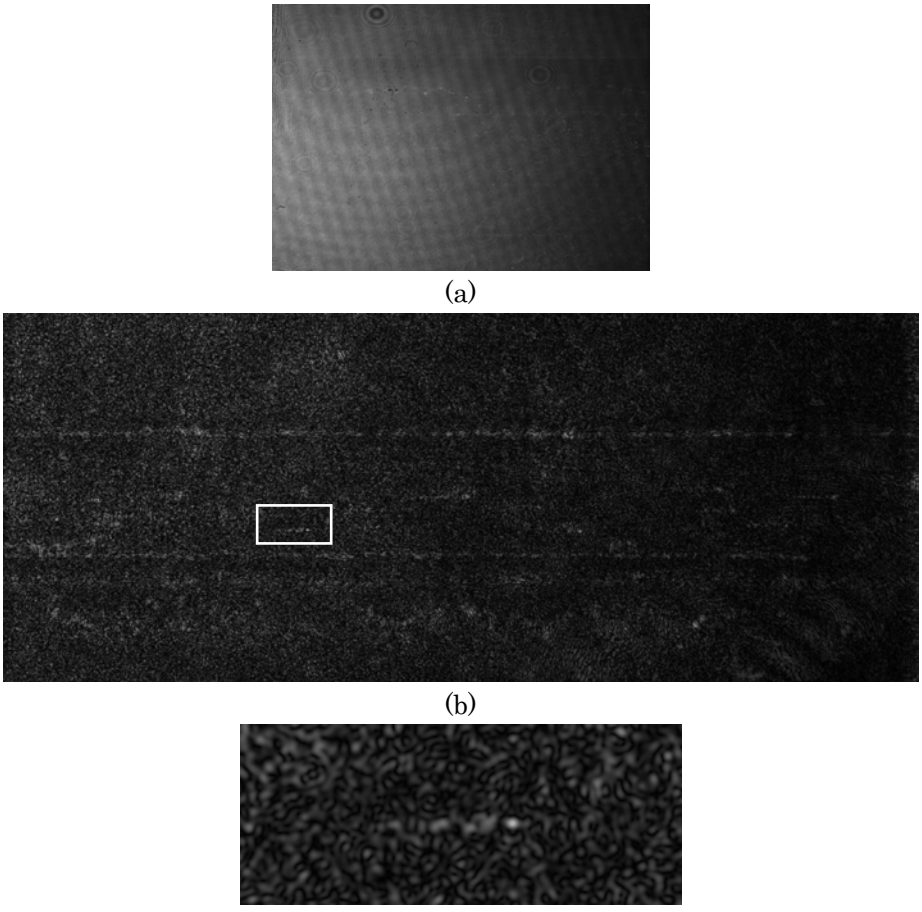

(a)

(b)

(c)

Figure 12. (a) Typical hologram. (b) Sum of intensities for a 10-hologram trace. Holograms were propagated for z=-0.07mm. (c) Zoomed area from (b).

It was found that the traces of the particles were not in focus in the selected plane, as it was expected if the capillary had a continuous laminar flow. That results indicated that particles were moving along the Z-axis too or the capillary had been fixed on the microscope at an angle.

For the following calculation, every hologram complex amplitude is propagated to the best-focussed plane. The first particle of the focussed trace was reconstructed at z=-0.065mm and the last one at z=-0.055mm. The intensity of the image particles in their best-focus plane are added and presented in Figure 13(a). In Figure 13(b) it is presented the zoomed area corresponded to the particle trace noted from the previous figure.

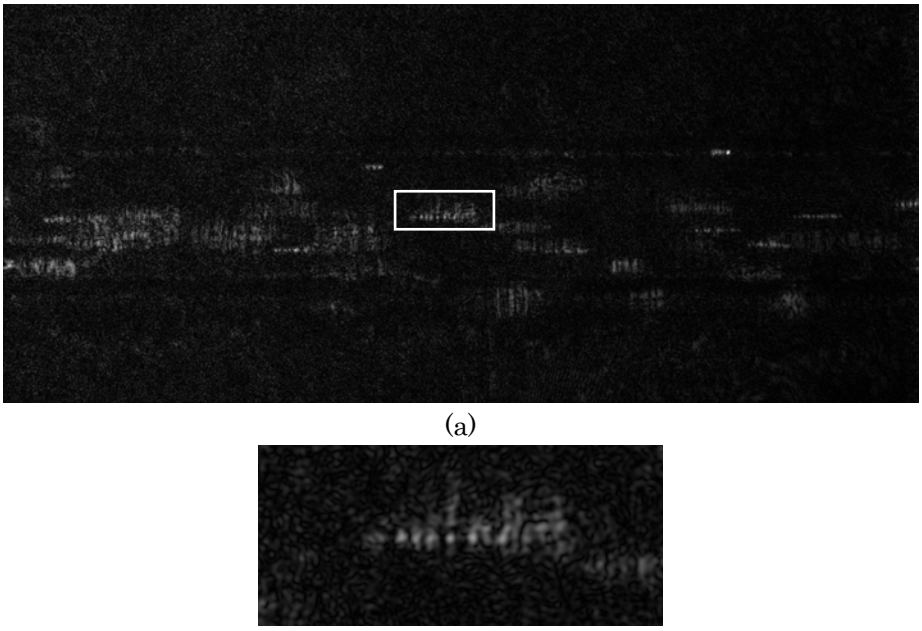

(a)

(b)

Figure 13. (a) Particle traces. Each hologram of the squared are has been propagated for a different Z. (b) Squared area from a1.

From measuring the displacement of the particles over the X-axis and the using the knowledge of the Z movement, the slope of the capillary is calculated giving an angle of 16.3º. This result do not match with our experimental possibilities.

To check the validity of this result, a reconstruction of the capillary using the calculated angle was performed. In the new routine the slope was corrected before propagating the particles in focus. Now, just a fraction of the recorded holograms was reconstructed, the capillary segment 2560x500 pixels. Now, instead of reconstructing single XY planes for a given Z, the total volume was reconstructed. To do so, the program propagates to different XY planes by using an array of, angle corrected, Z distances. A new complex amplitude 3D array was created with the reconstructed segment of the capillary. Now by representing the intensity of the array, it was possible to obtain a continuous trace of particles (for the given Z distance). However, as one can observe both edges of the capillary were deformed during the reconstruction (Fig. 14). A white dot line is represented in the figure below. Then, the idea of the capillary being tilted was discarded.

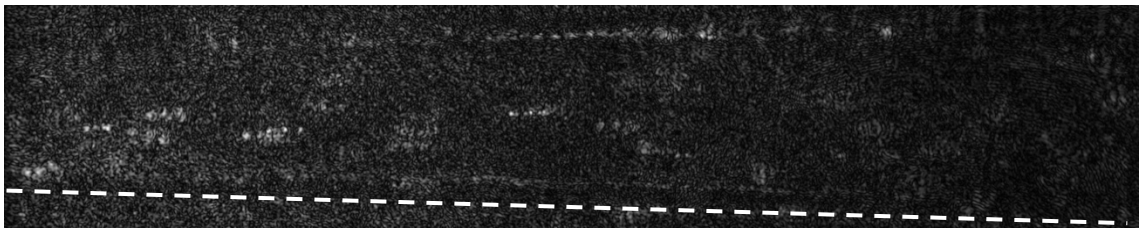

Figure 14. Capillary section reconstructed with the routine that corrects a slope angle.

The results show that the particles have movement in the plane, as expected, and also in the Z-axis. For a correct analysis, the XYZ position of each particle is required. Thus, 3D matrix containing complete information for different positions in Z was generated. To minimize computational time, just the section in which a single particle trace is located was reconstructed. As volume information is reconstructed, it is possible to present the traces of the particles along the XY plane together with the XZ plane. In the XY plane, the sum of the focussed particle images are presented. In the XZ plane, the scattering diffraction of the particles show the typical cigar shape distribution.

Furthermore, it is possible to compare this plot with the XY plane observing that the reason of the particle getting out of focus over the traces is that is going down in the Z direction.

Three different methods of representing the intensity of the particle traces were checked. In the first one, the absolute value of the sum of complex amplitudes of each hologram was plotted.

$$\phi'_a = abs[\sum(\phi(r,t))] \quad \textbf{(4)}$$

As one could expect, the imaginary terms of each amplitude interfere with each other resulting in background noise (Fig. 15(a, b)).

Then, the absolute value of each complex amplitude was summed resulting on a real array. Now, all the interference generated before with the complex terms disappeared. However, there was still some background noise.

$$\phi'_b = \sum[abs(\phi(r,t))] \quad \textbf{(5)}$$

Using this representation, some of the background noise from the previous figures was eliminated.

Finally, it was seen that the best method for representing a trace of particle was to sum the squared complex amplitudes of each of the propagated holograms.

$$\phi'_c = \sum(\phi(r,t))^2 \quad \textbf{(6)}$$

By summing the squared amplitudes, the intensities of the brightest points became higher so the particles can be observed better (Fig. 15(c, d)).

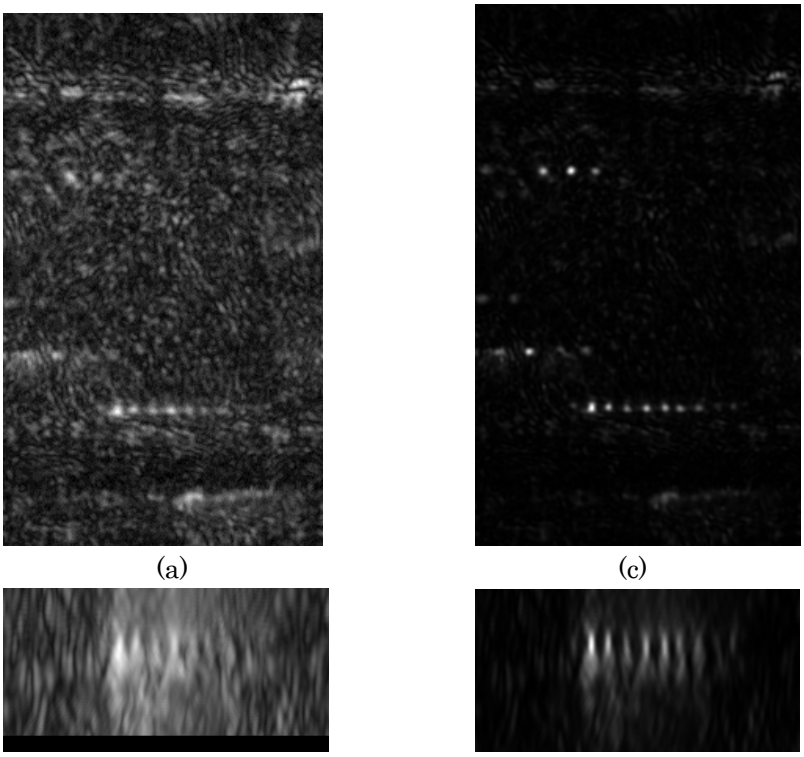

Figure 15. Digital reconstruction of the trace of a particle located at Z=-0.1mm.
Representation of the absolute value of the sum of complex amplitudes: (a) XY plane and (b) XZ plane.
Representation of the sum of the squared complex amplitudes of each propagated holograms: (c) XY plane and (d) XZ plane

While analyzing the complete capillary, a 3D information of the particle is obtained. The representation in XY planes, in which the intensity of each focussed particle is clearly plotted, hide the Z information. However, representing together the XY plane and the XZ plane, it was possible to distribute the particle motion over the Z-axis (Fig. 16).

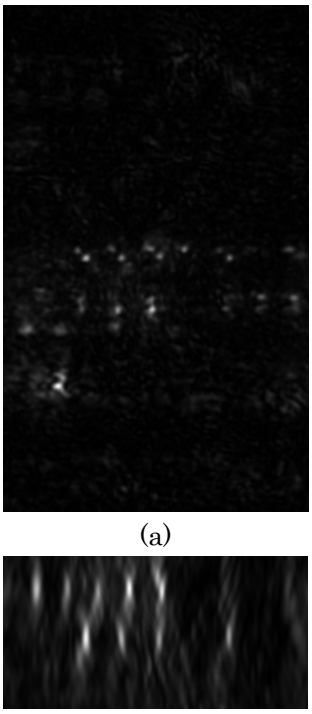

(a)

(b)

Figure 16. Digital reconstruction of the trace of different particles. Propagated at a distance Z=-0.13mm. As it is posible to obseve in the reconstruction of the XZ plane, two different traces appeared over the Z-axis.

Finally, the total area of the capillary has been reconstructed with this new method. Both XY and XZ planes are represented together in Figure 17. Series of particles are perfectly observed along the capillary and could be used for to measure the velocities. Notice that due to the particle scattering properties the resolution for the in-plane velocity is higher than in the Z direction.

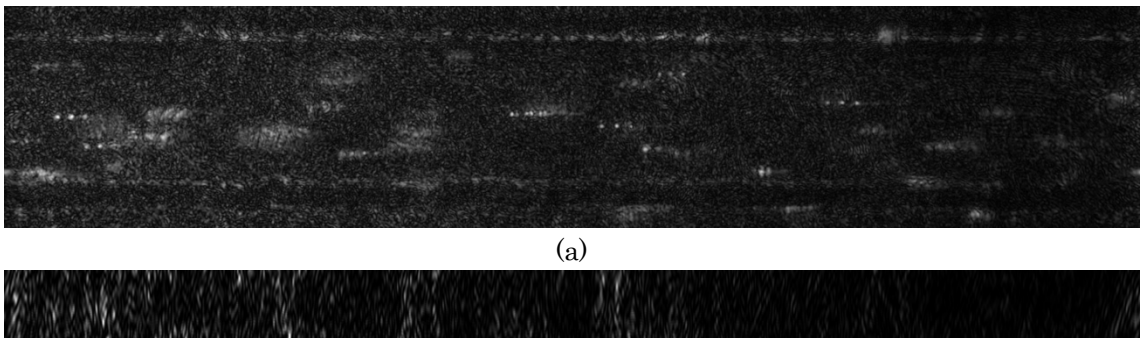

(a)

(b)

Figure 17. XY (a) and XZ (b) reconstruction of the capillary.

Once all the analysis of the data was performed, it was observed that still with the new method there were significant differences between the intensities of the different holograms used in the reconstruction. Specifically, it was seen that the first point of the trace rarely appeared in the reconstructions. It was figured it out by observing directly the intensities of

the registered holograms that the intensity of the reference beam was not continuous but changed over time. Consequently, the proportion of reference-object beam was not constant and could have been the reason some of the particle over the trace disappeared. Later on, it was verified by the reconstruction of the first hologram. In that case the first particle did appear.

According to the flow direction of the circuit commanded by the pump, the liquid should have flown right to left. However, once all the recording of data was performed and the holograms were analysed we realized that the liquid was flowing in the opposite direction. The possible reason was pressure differences between the pump, the capillary and the beaker. Then, particle motion was recorded moving left to right. As the main objective of the project was to observe the motion and trace particles, this is considered as a first-time-use mistake and a smaller syringe has been designed for further studies.

4. Conclusions

During this work, a new experimental set-up has been designed and implemented to measure the position and velocities of magnetic particles inside a glass capillary. Different capillaries were designed and manufactured by the start-up BeOnChip and, for this project a 100-micrometer channel was used for the experimental recording of data.

An of-axis DHM set-up has been designed for this purpose. To check aligment and magnifications of this set-up, arrays of microlenses were recorded. Furthermore, the reconstruction of the complex object wave at any Z-position has been calculated. Then, in order to implement a microfluidics system and register particles moving through it, holograms of a sample containing a 1mm channel were recorded.

Finally, DHM technique has been applied to measure in the new 100-micrometer width capillary. The microchannel has been filled with a mixture of water and glycerine containing 3-micrometer diameter magnetic particles. Series of holograms were recorded. Remark that the whole volume of the capillary was recorded.

The numerical analysis of the holograms propagated the complex amplitude to different planes has been performed. Different ways of analysis has been done and the results were presented.

A new visualization of the results showing the XY plane and the XZ plane are presented. In the XY representation the image of the particles moving through the system are observed. In the XZ, the diffraction pattern of the particles (cigar shape) was shown. In both cases the corresponding velocities could be calculated. Due to the diffraction pattern in the Z-direction, the accuracy in the Z-position detection of the particles with this technique is always worse than in-plane localization.

The next step will be applied the technique to measure the movement of particles inside the capillary under the influence of a magnet. A new microfluidics system will be implemented with the objective of measuring and controlling the flow over the circuit. For that reason, a new syringe will be used and the differences of pressure over the system will be analysed before the recording of data.

References

[1] Masashige Shinkai, "*Functional magnetic particles for medical application"*, Journal of Bioscience and Bioengineering, vol 94, Issue 6, December 2002.

[2] Myung K. Kim, "*Principles and techniques of digital holographic microscopy",* SPIE Reviews 1(1), 018005, April 2010.

[3] D. Gabor, "*A new microscope principle"*, Nature, vol. 161, p. 777, 1948.

[4] U. Schnars and W. Jueptner, "*Digital Holography: Digital Hologram Recording, Numerical Reconstruction and Related Techniques"*, Berlin, Germany: Springer 2005.

[5] J. Burke, H. Helmers, C. Kunze, and V. Wilkens*, "Speckle intensity and phase gradients: influence on fringe quality in spatial phase shifting ESPI systems"*, Opt. Commun. 152,144–152 (1998).

[6] M. Özcan and M. Bayraktar, "*Digital holography image reconstruction methods*", Proc. SPIE 7233, 72330B, 3 February 2009.

[7] *BeOnChip. (https://beonchip.com/)*

[8] Chemyx, *Nexus 3000 High FlowSyringe* (https://www.chemyx.com/downloads/nexus-3000-technical-specs.pdf)